Available online at www.sciencedirect.com
ScienceDirect
Thermochimica Acta 463 (2007) 69–76
thermochimica acta
www.elsevier.com/locate/tca

Thermite reactions of Al/Cu core-shell nanocomposites with WO_3

Yi Wang[a], Wei Jiang[a], Zhipeng Cheng[a], Weifan Chen[b], Chongwei An[a],
Xiaolan Song[a], Fengsheng Li[a,*]

[a] *National Special Superfine Powder Engineering Research Center, Nanjing University of Science & Technology, Nanjing 210094, China*
[b] *School of Materials Science & Engineering, Nanchang University, Nanchang 330031, China*

Abstract

The Al/Cu core-shell nanocomposites are fabricated via a facile displacement method and characterized by scanning electron microscopy (SEM) and energy dispersion spectrometry (EDS). In comparison with the thermite reactions of bulk Al powders with WO_3, the thermite reactions of Al/Cu core-shell nanocomposites with WO_3 as a function of the equivalence ratio of Al to WO_3 (Φ) and reaction environment are investigated by differential scanning calorimetry (DSC) and dealt with in terms of reaction performance of thermite including onset and peak temperatures, maximum reaction rate (Q_{max}) and reaction heat (ΔH_r) based on DSC data. The results indicate that the reactivity of Al/Cu core-shell nanocomposites with WO_3 is higher than that of bulk Al powders but depends strongly on the equivalence ratio, which is optimal when the fuel in the thermites is slightly rich, i.e. $\Phi = 1.2$. It is significant that in air, ΔH_r of WO_3 and core-shell Al/Cu ($\Phi = 1.2$) is higher than that of WO_3 and bulk Al by 49%. In addition, it is also observed that the solid phase reaction $2Al(s) + WO_3(s) = Al_2O_3(s) + W(s)$ may be irritated prior to Al melting when heating Al/Cu–WO_3 in argon, which is confirmed by DSC and X-ray diffractometry (XRD). Finally, the reasons of improving the thermal performance of thermites have been discussed.

Keywords: Thermite reactions; Al/Cu core-shell nanocomposites; Al powders; WO_3; Thermal reactivity

1. Introduction

Thermite reactions can be described as exothermic reactions involving the reduction of metallic oxides with aluminum or other activated metal powders. This kind of reaction can be generalized into:

$$M + AO_x = MO_x + A + \Delta H \tag{1}$$

where M is a metal and A is either a metal or a non-metal, MO_x and AO_x are their corresponding oxides, and ΔH is the heat generated by the reaction. Because of the large exothermic heat, a thermite reaction can generally be initiated locally and then become self-sustaining, a feature, which makes full use of their energy. These reactions have been utilized in reactive fill for enhanced warhead projectiles, high performance additives for solid rocket propellants, lead-free electric matches and a host of other application [1–6]. As composite energetic materials, the preparation of thermites is distinct from the monomolecular energetic materials. For the thermites in specific application, desired thermal properties can be readily tailored by varying ratios of oxidizer to fuel. However, due to the granular nature of composite energetic materials, reaction kinetics largely depends on mass transport rates between reactants [7,8]. Although the composites may have extremely high energy density, the released energy is generally below their theoretical values. It is well known that the initiation abilities and detonation performance of energetic materials are strongly influenced by their microstructures [9,10]. For example, when the size of Al or metallic-oxides powders fall within nanoscale, these thermites will have higher reactivity and burning rates than those containing micron-sized components due to more intimate contact between nanometer components [11,12]. However, it is very difficult to fabricate nanometer Al powders on a large scale because of cost, safety, process, etc. In our previous study [13], we dealt with the fabrication of the Al/Cu core-shell nanocomposites via a displacement method, which is facile and productive. Here we investigate the thermite reactions of Al/Cu core-shell nanocomposites with WO_3 and compare them with those of micron-sized

---

[*] Corresponding author. Tel.: +86 25 84315942.
E-mail address: wangyi528528@yahoo.com.cn (F. Li).

0040-6031/$ – see front matter © 2007 Elsevier B.V. All rights reserved.
doi:10.1016/j.tca.2007.07.017

Al powders with WO_3 with respect to the thermal performance. As partial film of Al_2O_3 on the surface of micron-sized Al particles is replaced by layers of Cu nanoparticles in the synthesis of Al/Cu nanocomposites, a kind of novel thermites of Al/Cu core-shell nanocomposites and WO_3 possessing high reactivity can be obtained.

2. Experimental

2.1. Materials

The bulk Al powders (with 99% purity, average particle size $d_{50} = 5\,\mu m$) were purchased from Anshan superfine powders Ltd., China. $CuSO_4{\cdot}5H_2O$ (A.R.), NH_4F (C.P.), gelatin (C.P.) and sodium diethyldithiocarbamate trihydrate (SDT) (A.R.) are obtained from Beijing chemical Ltd., China. The WO_3 powders (with 99.99% purity, average particle size $d_{50} = 12\,\mu m$) and sodium dioctylsulfosccinate (SDS) (C.P.) are purchased from Shanghai chemical Ltd., China.

2.2. Fabrication of Al/Cu core-shell nanocomposites and preparation of the thermites

The core-shell Al/Cu nanocomposites were fabricated via a displacement method because $E^{\theta}_{Al^{3+}/Al}$ (−1.66 V) is quite lower than $E^{\theta}_{Cu^{2+}/Cu}$ (+0.34 V) [13]. The designed mass fraction of Cu to the whole Al/Cu nanocomposites is 3 wt.%. As a protective agent of active Al, the gelatin solution with proper concentration was introduced to $CuSO_4{\cdot}5H_2O$ solution. After the pH value of the solution was adjusted at about 6.4, Al powders ultrasonicated in cool distilled water were rapidly added into the above-mentioned solution kept at 35 °C. Then NH_4F solution was tardily dripped into Al suspension to remove the Al_2O_3 layers on the surface of Al powders until the suspension cannot change the color of SDT. After filtration, lavation and evaporation in vacuum at 40 °C, the Al/Cu core-shell nanocomposites were fabricated.

In the present study, the stoichiometric thermite reaction can be expressed as the following equation [1]:

$$2Al + WO_3 = Al_2O_3 + W \tag{2}$$

The equivalence ratio Φ for this reaction is calculated according to [14]:

$$\Phi = \frac{(F/O_x)_{\text{Actual}}}{(F/O_x)_{\text{Stoichiometric}}} \tag{3}$$

where F represents the mass of fuel (Al), O_x the mass of oxidizer (Al_2O_3).

The thermites were prepared by mixing the fuel and oxidizer in the required proportions. With 1.5 wt.% SDS added, the mixtures of the fuel (Al or Al/Cu nanocomposites) and WO_3 powders at the desired equivalence ratio Φ were ultrasonicated in *n*-hexane, then heated at low temperature in vacuum to evaporate *n*-hexane and finally sifted through a wire mesh of 200-μm to obtain the thermites used for investigation.

2.3. Sample characterization

The morphology and surface element of the samples were examined by a LEO-1530VP field-emission scanning electron microscope coupled with energy dispersive spectroscopy (OXFORD, INCA-300). Differential scanning calorimetry of the thermites was performed on a TA Model Q600 differential scanning calorimeter from room temperature to 1100 °C under the air or argon gas flowing at 10 mL/min. The thermites of about 3 mg were contained in open alumina pans. Heating rate of 5, 10 and 20 °C/min was adopted. The phase variations of the thermites in the heating process were investigated via a Bruker Advance D8 X-ray diffractometer, using Cu Kα radiation at 40 kV and 30 mA.

3. Results

3.1. Characterization of the samples

As shown in Fig. 1(a), raw Al particles are spherical in shape and smooth on the surface except few tiny Al grains, whereas the surface of the particles shown in Fig. 1(b) are covered with spherical particles. It can be seen more clearly in Fig. 1(c) that the surface of the arrow-pointed large particle shown in Fig. 1(b) is deposited by the tightly agglomerated nanoparticles of 20–30 nm in size, showing honeycomb-like coarse surface. When as-prepared Al/Cu core-shell nanocomposites are immersed into diluted hydrochloric acid until there is no effervescence, the porous shell-shaped products can be obtained, as revealed in Fig. 1(d). It is more clear in Fig. 1(e) that the etching-obtained spherical particles are hollow and composed of agglomerated nanoparticles. To detect the surface element of Al/Cu core-shell nanocomposites before and after etching, EDS measurements were carried out. Fig. 2 is EDS spectra of Al/Cu nanocomposites before and after etching. It indicated that the surface of Al/Cu nanocomposites contains Cu and Al. Due to the relative low fraction (3 wt.%) and the thinner shell of Cu, the presence of Al element was made clear. However, the element of Cu is dominant. For Al/Cu nanocomposites after etching, only Cu element is present and the Al element is removed. It can be concluded that Al/Cu nanocomposites with micron-sized Al particle in the core and Cu nanoparticles as the shell can be prepared by the displacement method [13].

3.2. DSC analysis of the thermites

Fig. 3 shows DSC curves of Al–WO_3 with different equivalence ratio Φ recorded both in air and in argon. In each curve, the endothermic peak at about 660 °C, i.e. the theoretical melting point of aluminum [15,16], is observed and may be associated with the melting of aluminum. The exothermic peaks are located at 993–1056 °C, which represents the thermite reaction of Al with WO_3. Apparently, the figures of these peaks vary with the atmosphere changes. In air, each DSC curve shows just one exothermic peak. When the reaction atmosphere is converted from air to argon, these curves present three exothermic peaks, corresponding to three stages in the thermite reaction. It can also

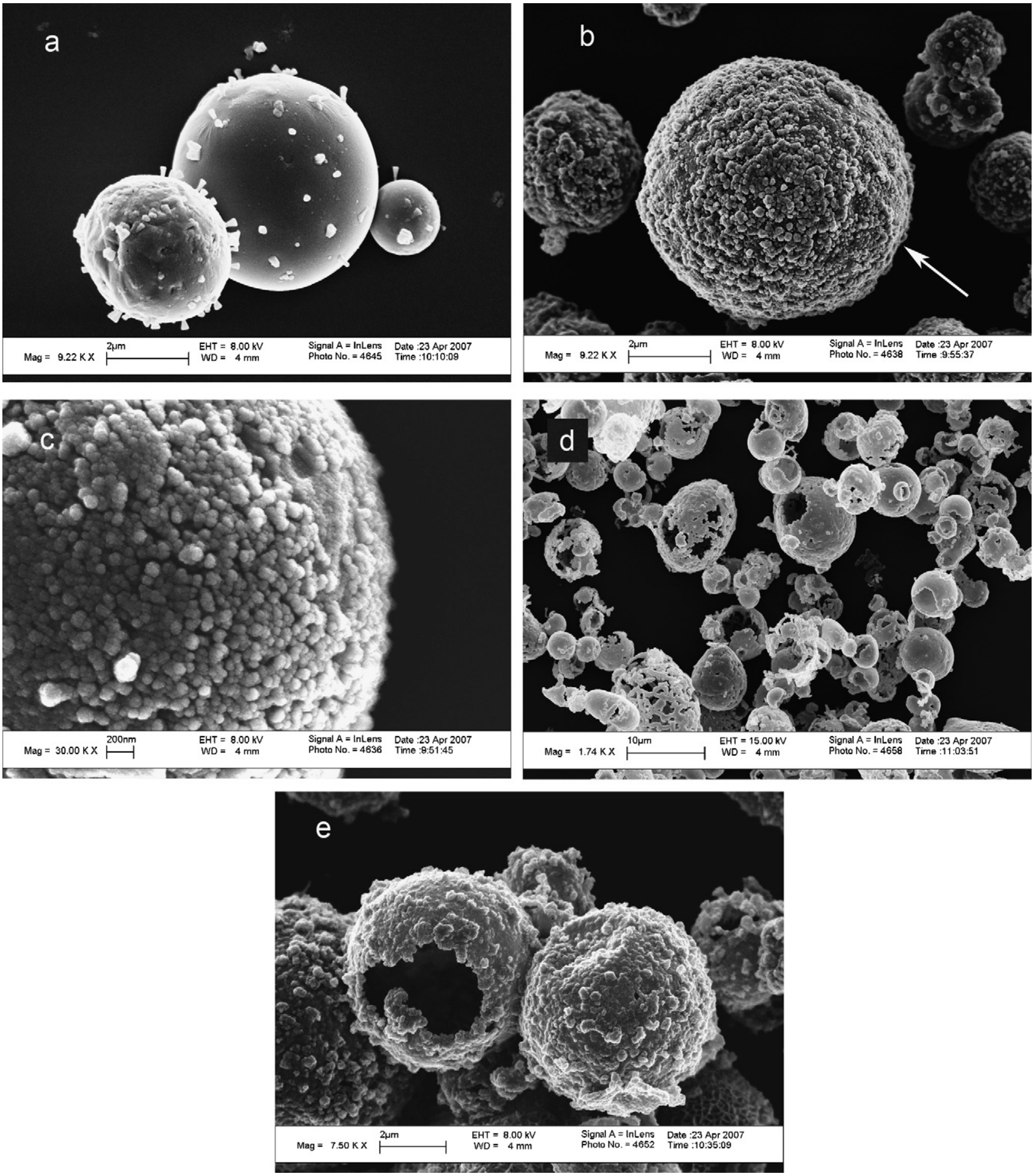

Fig. 1. SEM micrographs of (a) raw Al particles; (b) Al/Cu core-shell nanocomposites prepared by the displacement method; (c) partial surface of the arrow-pointed particle shown in Fig. 1(b); (d) products obtained by etching Al/Cu core-shell nanocomposites with diluted hydrochloric acid; (e) products shown in Fig. 1(b) at higher magnification.

be observed from Fig. 3 that the correspondent exothermic peak of Al–WO_3 at different equivalence ratio Φ appears at higher temperature in air than in argon.

Fig. 4 presents DSC curves of core-shell Al/Cu–WO_3 with different equivalence ratio Φ recorded under the different flowing atmosphere. As is demonstrated in Fig. 4(a), when the thermite reaction for Al/Cu–WO_3 occurs in air, DSC curves almost level off in the temperature range of 400–850 °C and only in the intercepted DSC curves on enlarged scale can the endothermic peak assigned to Al melting at about 660 °C be observed, whereas the only exothermic peaks ranging from 906 °C to 988 °C in each DSC curve are attributed to thermite

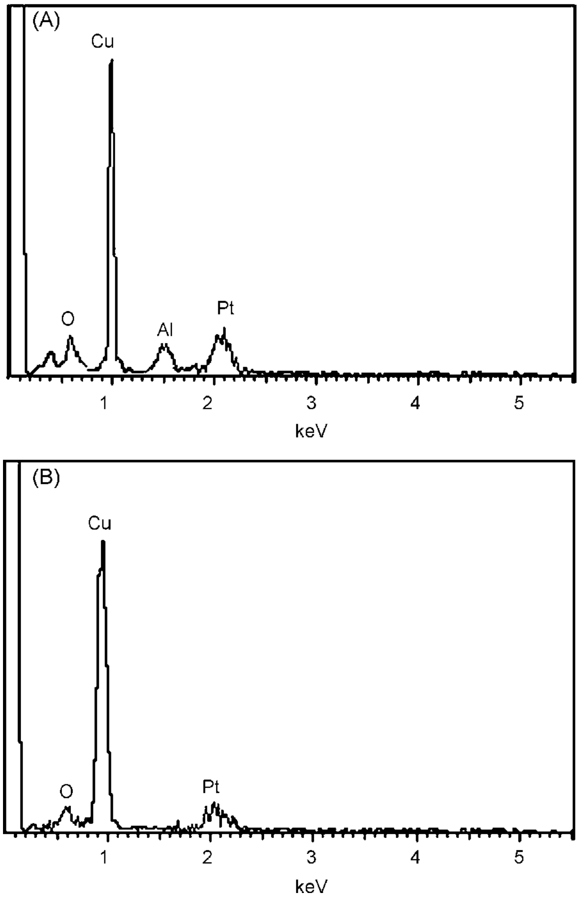

Fig. 2. EDS spectra for (A) Al/Cu core-shell nanocomposites prepared by a displacement method; (B) products obtained by eroding Al/Cu core-shell nanocomposites with diluted hydrochloric acid.

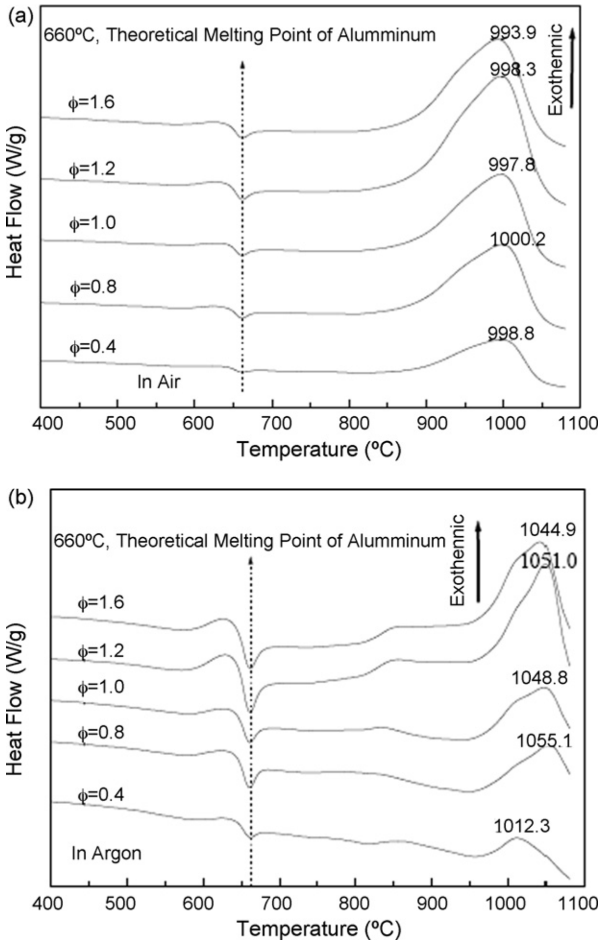

Fig. 3. DSC curves of Al–WO_3 with different equivalence ratio Φ at heating rate of 20 °C/min, respectively, recorded (a) in air and (b) in argon.

reaction for Al/Cu–WO_3. In sharp contrast, when the atmosphere is converted from air to argon, three exothermic peaks and one endothermic peak in the curves for Φ range from 0.8 to 1.6 can be observed, as shown in Fig. 4(b). Interestingly, one weak exothermic peak, which is more apparent in the intercepted DSC curves in Fig. 4(b), appears prior to Al melting and hence may be related to some solid phase reaction. This finding will be discussed in more detail subsequently. In addition, for Al/Cu–WO_3 in argon, the exothermic peaks broaden and appear at higher temperature compared with those in air.

3.3. *Thermal performance analysis of thermite reactions*

Onset and peak temperatures of Al–WO_3 and core-shell Al/Cu–WO_3 as a function of equivalence ratio are presented in Fig. 5. It can be seen that in the most cases, variation in Φ for each Al–WO_3 and core-shell Al/Cu–WO_3 has few effects on the onset and peak temperatures whether in air or in argon. As shown in Fig. 5(a), in air, the average value of onset temperatures of Al/Cu–WO_3 at different equivalence ratios is higher than that of Al–WO_3 by 31.7 °C, while the average value of peak temperature of Al/Cu–WO_3 is lower than that of Al–WO_3 by 77.04 °C. Moreover, the average variation value of Al/Cu–WO_3 from onset temperature to peak temperature (5.7 °C) is lower than that of Al–WO_3 (114.4 °C) by 108.69 °C. All these suggest that Al/Cu–WO_3 in air is a more passive energetic material but has more concentrative exothermic course than Al–WO_3. From Fig. 5(b), in argon, the average values of onset temperatures for two thermites are almost equal while the average value of peak temperature of Al/Cu–WO_3 is lower than that of Al–WO_3 by 59.2 °C. In summary, compared with Al–WO_3, whether in air or in argon, Al/Cu–WO_3 is more passive but much more concentrative in terms of energy release and may be used as a novel kind of passive and effective energetic materials for some specific martial applications, such as projectiles, energetic-shaped charge, active fragments, detonator, etc.

The reaction heats for Al–WO_3 and core-shell Al/Cu–WO_3 in air and in argon can be obtained from the integrated heats of the exothermic peaks in DSC curves. The results are shown in Fig. 6 as a function of equivalence ratio Φ. It can be seen that the reaction heats of Al/Cu–WO_3 are generally higher than those of Al–WO_3 systems and arrive at the maximum for the slightly fuel rich ($\Phi = 1.2$) mixture whether in air or in the argon. However, all measured reaction heats are considerably lower than the theoretical value (2910 J/g) [17]. It is worth noting that the reaction heat in air for Al/Cu–WO_3 with $\Phi = 1.2$ is larger than that for Al–WO_3 by 56% and accounts for approximately 86% of the theoretical value. As is shown in Fig. 6(a and b), when the

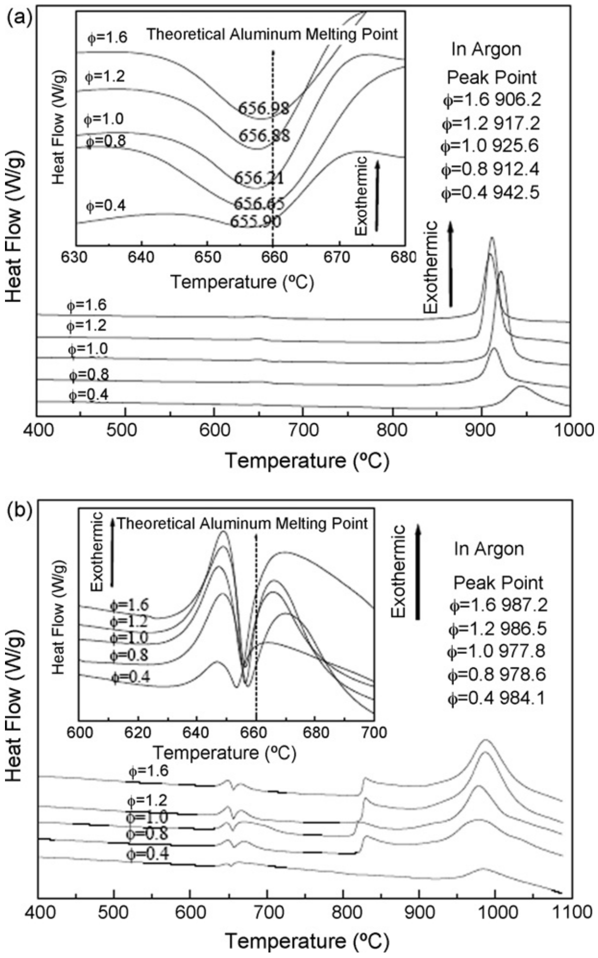

Fig. 4. DSC curves of core-shell Al/Cu–WO_3 with different equivalence ratio Φ at heating rate of 20 °C/min, respectively, recorded (a) in air and (b) in argon. Inserted graphs are the intercepted DSC curves on enlarged scale.

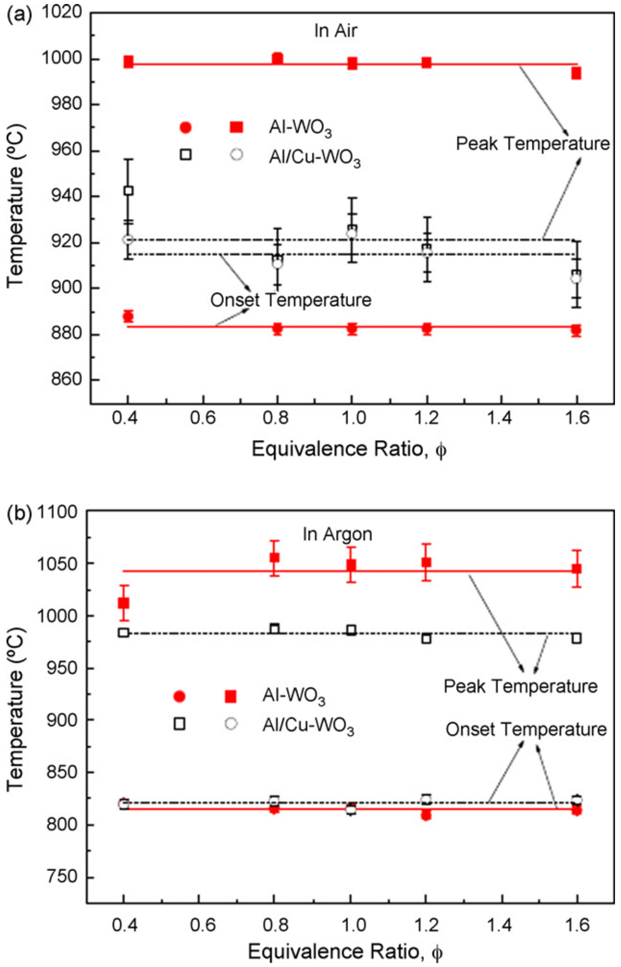

Fig. 5. The onset and peak temperatures of Al–WO_3 and core-shell Al/Cu–WO_3 (a) in air and (b) in argon as a function of equivalence ratio Φ. The values plotted and error bars are the average and standard deviation, respectively, of the temperature obtained at different equivalence ratio. The dashed and solid lines are only intended to show the average of onset or peak temperatures.

atmosphere is converted from air to argon, the reaction heats for Al–WO_3 and core-shell Al/Cu–WO_3 at investigated equivalence ratio are dramatically reduced, for example, the reaction heats in air for core-shell Al/Cu–WO_3 is 2508 J/g, for Al–WO_3 1169 J/g. Sun et al. [18] reported that due to the incompleteness of the thermite reactions, the reaction heats for metastable intermolecular composites (MIC) which consist of a nano-sized Al-MoO_3 systems are approximately 35% of the theoretical value.

The maximum reaction rate per gram of aluminum reacted in air and in argon for Al–WO_3 and core-shell Al/Cu–WO_3, which is determined by the heat flow rate at the dominant exothermic peak of Al–WO_3 and Al/Cu–WO_3, is plotted against equivalence ratio Φ. As shown in Fig. 7(a and b), whether in air or in argon, the values of $Q_{\max}$ for Al/Cu–WO_3 are generally higher than those for Al–WO_3 and reach their respective maximum at $\Phi = 1.2$. Remarkably, in air, the maximum reaction rate at $\Phi = 1.2$ has a more than 10-fold increase from 6.95 W/g for Al–WO_3 to 84.91 W/g for Al/Cu–WO_3, whereas for Al–WO_3 and Al/Cu–WO_3 in argon, their maximum reaction rates have little difference. Furthermore, the maximum reaction rate for Al–WO_3 and Al/Cu–WO_3 is considerably higher in air than in argon. In summary, the reactivity of Al/Cu nanocomposites with WO_3 is considerably higher than those of bulk Al particles under the same conditions, especially in air.

4. Discussion

Comparing two inserted graphs in Fig. 4, it can be easily observed that exothermic reaction of Al/Cu–WO_3 in argon occurs prior to Al melting point, suggesting presence of some solid–solid state reaction. These reactions did not complete before reaching the melting point of Al. Therefore, the heats of these reactions are inaccurate due to the competing positive and negative energy signals. This phenomenon indicates that partial Al/Cu nanocomposites have been partially oxidized by WO_3 in argon before the primary thermite reaction occurs.

To further confirm the possible solid state reaction prior to Al melting, we collected the quenched products obtained by heating the thermites to 700 °C both in air and in argon, and then conducted a XRD analysis. Fig. 8 shows the XRD patterns of the quenched products. As is indicated in Fig. 8, the peaks of W and Al_2O_3 appear in the XRD pattern for Al/Cu–WO_3 in argon

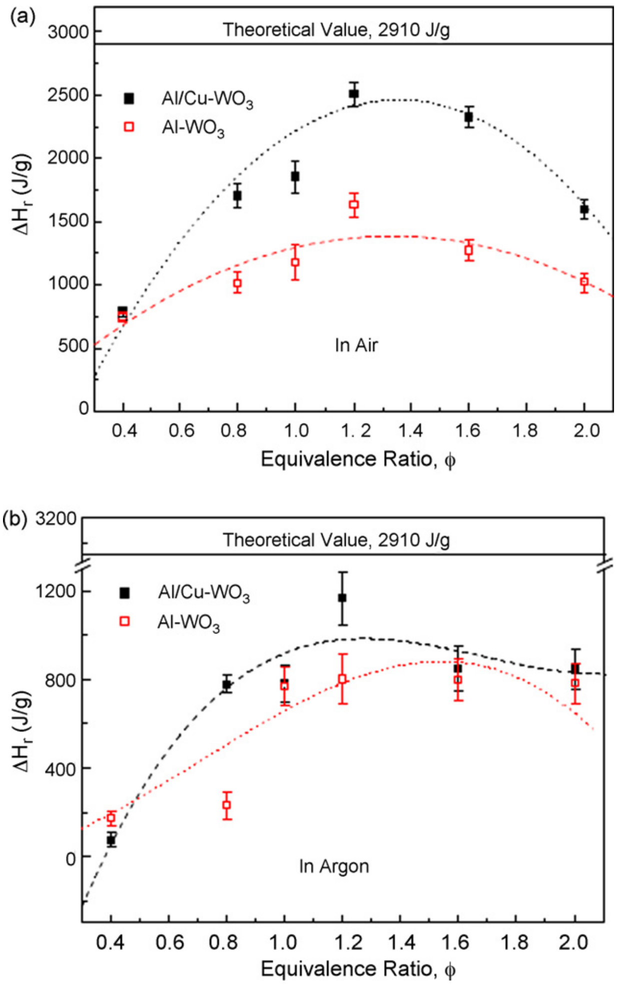

Fig. 6. Reaction heats for Al–WO_3 and core-shell Al/Cu–WO_3 (a) in air and (b) in argon as a function of equivalence ratio Φ. The values plotted and error bars are the averages and standard deviations, respectively, of the reaction heat obtained at the heating rates of 5, 10 and 20 °C/min. The dashed and doted lines are only intended to show the trends of data.

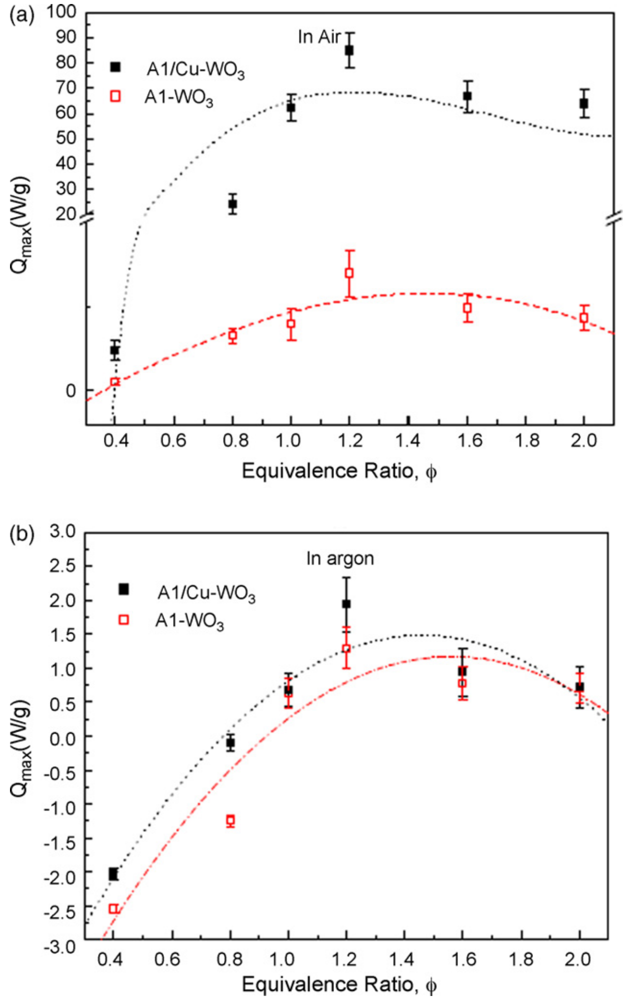

Fig. 7. Maximum reaction rates for Al–WO_3 and core-shell Al/Cu–WO_3 (a) in air and (b) in argon as a function of equivalence ratio Φ. The values plotted and error bars are the averages and standard deviations, respectively, of the reaction heat obtained at the heating rates of 5, 10 and 20 °C/min. The dashed and doted lines are only intended to show the trends of data.

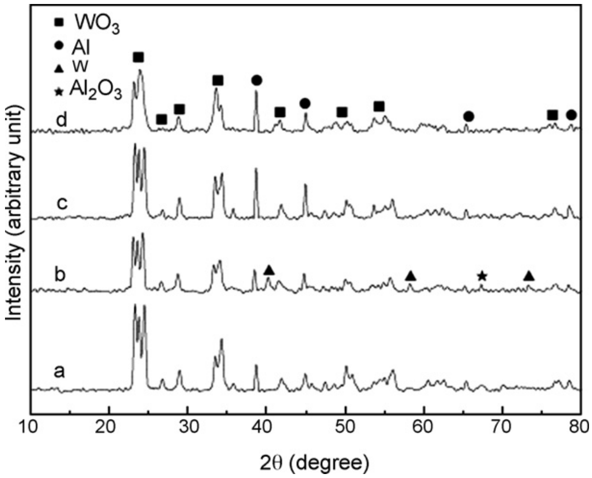

Fig. 8. XRD patterns for the reaction products obtained by heating the $\Phi = 1.2$ different thermites to 700 °C and quenching under different atmosphere: (a) Al–WO_3 in argon; (b) Al/Cu–WO_3 in argon; (c) Al–WO_3 in air; (d) Al/Cu–WO_3 in air.

whereas in other three patterns, just peaks of WO_3 and Al can be noted. It is also observed that the peak intensities for starting materials WO_3 and Al shown in the pattern (b) decrease compared with other three patterns. However, the peak intensities of the reaction products (e.g. W and Al_2O_3) are fairly faint due to this short-time reaction. Combined with the exothermic peak in the range of 640–650 °C shown in Fig. 4(b), the above XRD results also confirm that the existence of the solid state reaction, i.e. $2Al(s) + WO_3(s) = Al_2O_3(s) + W(s)$.

In general, each Al particle was enwrapped by a dense Al_2O_3 layer. As the heating is proceeding, Al_2O_3 layer will shrink due to the 20% density increase resulted from phase transformation from amorph-Al_2O_3 to γ-Al_2O_3 and active Al is exposed [19]. For Al–WO_3 system, the melt Al will flood from fracted Al_2O_3 shell, contact with WO_3 and lead to occurring of the thermite reaction. As a result, a new dense Al_2O_3 layer forms and gets thicker and thicker. If this oxide layer were not broken again, the reaction would cease before the total mass of Al core is consumed completely. For Al/Cu–WO_3 system, however, each Al/Cu core-shell nanocomposite has many Cu nanoparti-

Table 1
Thermites and their reaction heats

Thermite no.	$\Phi = 1.2$ Thermite components excluding WO_3	Heats of reaction, ΔH_r (J/g)
T1	Al powders	805.4
T2	Mixture of 3wt.% Cu nanoparticles and 97wt.% Al powders	838.6
T3	Al/Cu nanocomposites prepared via a displacement method	1198

cles on the surface of Al particle, which replace bulk of Al_2O_3 layer. This will result in the intimate contact between nanometer Cu particles and active Al core and largely increase the specific surface area of Al particles. Meanwhile, these nanometer Cu particles will act as many active centers in the course of thermite reaction. Therefore, it is the unique microstructure of Al/Cu core-shell nanocomposites may improve the performance of thermite reaction in Al–WO_3 system.

To further investigate effect of microstructure of Al/Cu core-shell nanocomposites on reactivity of thermite reaction for Al/Cu–WO_3, we prepared a thermite by mixing 3 wt.% Cu nanoparticles and 97 wt.% raw Al particles with WO_3 in proportion of $\Phi = 1.2$ and made a comparative study on three thermites including the as-prepared thermite via DSC analysis. Three thermites and their reaction heats are summarized in Table 1. DSC curves of the thermites listed in Table 1 are shown in Fig. 9.

According to our previous research, synthesis of Al/Cu core-shell nanocomposites via a displacement method is based on the following reactions

$$Al_2O_3 + 6H^+ \rightarrow 2Al^{3+} + 3H_2O \tag{4}$$

$$Al^{3+} + 6F^- \rightarrow [AlF_6]^{3-} \tag{5}$$

$$2Al + 3Cu^{2+} \rightarrow 2Al^{3+} + 3Cu \tag{6}$$

Firstly, Al_2O_3 layer on the surface of raw Al particles is removed in acid solution to produce Al^{3+}, and then NH_4F is added into solution and the stable complex $[AlF_6]^{3-}$ is formed. As a result, the balance of the reaction (4) move rightward and removal rate for Al_2O_3 is accelerated. Only when Al_2O_3 layer on the surface of raw Al particles is removed to expose the active Al, Cu^{2+} in solution can be reduced into nanometer Cu particles. Therefore, the Al/Cu core-shell nanocomposites obtained via the displacement method almost do not contain Al_2O_3 layer.

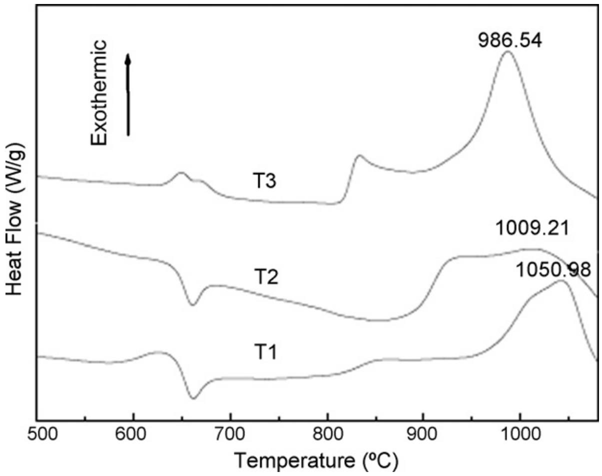

Fig. 9. DSC curves of the thermites listed in Table 1, recorded in argon at heating rate of 20 °C/min.

As showed in Table 1 and Fig. 9, in spite of the almost same mass fraction of Cu nanoparticles as T3, T2 has lower reaction heat and higher peak temperature, which is due to the fact that Al_2O_3 layer on the surface of raw Al particles prevents Cu nanoparticles from intimate contact with active Al, whereas in preparation process of Al/Cu core-shell nanocomposites via the displacement method, Al_2O_3 layer on the surface of raw Al particles is removed to expose the active Al particles, which are subsequently deposited by Cu nanoparticles resulting from reduction reaction between Al and Cu^{2+}. Thus, T3 has the lowest peak temperature and the highest reaction heat owing to its peculiar core-shell structure.

5. Conclusions

SEM images and EDS spectra indicate that Al/Cu core-shell nanocomposites can be prepared via a facile displacement method and that 20–30 nm Cu nanoparticles have been deposited on the surface of raw Al particles successfully. The analysis of DSC shows that based on onset and peak temperatures, maximum reaction rate (Q_{max}) and reaction heat (ΔH_r), the reactivity of Al/Cu–WO_3 both in air and in argon is higher than that of Al–WO_3 but depends strongly on the equivalence ratio Φ, which is optimal when the fuel in the thermites is slightly rich, i.e. $\Phi = 1.2$. Moreover, the atmosphere of thermite reaction has great influence on reactivity. Remarkably, the reactivity of Al/Cu–WO_3 in air is enhanced by large. It is also observed that the solid phase reaction $2Al(s) + WO_3(s) = Al_2O_3(s) + W(s)$ may be irritated prior to Al melting when heating Al/Cu–WO_3 in argon, which is confirmed by DSC and XRD. Finally, the reasons of increase in the reactivity of thermites are discussed. We consider that it is the unique microstructure of Al/Cu core-shell nanocomposites that leads to a great improvement in the reactivity for Al/Cu–WO_3.

Acknowledgements

This work is the combination of several research groups in our center. The authors would like to thank Chengfang Che of National Special Superfine Powders Engineering Research Center in Nanjing University of Science & Technology for her enthusiastic support in DSC analysis and Dr. Edward L. Dreizin of New Jersey Institute of Technology who provided many helpful suggestions for our experiments.

References

[1] R. Ricceri, P. Matteazzi, J. Alloy Compd. 358 (2003) 71–75.
[2] N. Uzunov, R. Ivanov, Appl. Surf. Sci. 225 (2004) 72–77.
[3] K.W. Ciurowa, K. Gamrat, Z. Sawlowicz, J. Therm. Anal. Calorim. 80 (2005) 619–623.
[4] X.L. Zhe, C.A. Dioka, A. Hendry, J. Eur. Ceram. Soc. 25 (2005) 695–702.
[5] R.H. Fan, H.L. Lu, K.N. Sun, Thermochim. Acta 440 (2006) 129–131.

[6] S.M. Umbrajkar, M. Schoenitz, E.L. Dreizin, Thermochim. Acta 451 (2006) 34–43.

[7] J. Mei, R.D. Halldearn, P. Xiao, Scripta Mater. 41 (1999) 541–548.

[8] T.M. Tillotson, A.E. Gash, R.L. Simpson, J. Non-Cryst. Solids 285 (2001) 338–345.

[9] S. Valliappan, J. Swiatkiewicz, J.A. Puszynski, Powder Technol. 156 (2005) 164–169.

[10] T.M. Yue, K.J. Huang, H.C. Man, Surf. Coat. Technol. 194 (2005) 232–237.

[11] K.B. Plantier, M.L. Pantoya, A.E. Gash, Combust. Flame 140 (2005) 299–309.

[12] S. Majumdar, G.B. Kaleb, I.G. Sharma, J. Alloy Compd. 394 (2005) 168–175.

[13] Z.P. Cheng, Y. Yang, X.D. Liu, Acta Chim. Sinica 65 (2007) 81–85.

[14] J.J. Granier, M.L. Pantoya, Combust. Flame 138 (2004) 373–383.

[15] S.X. Wang, K.M. Liang, X.H. Zhang, J. Mater. Sci. Lett. 22 (2003) 855–856.

[16] L. Lin, Q.J. Xue, H.W. Liu, J. Inorg. Mater. 11 (1996) 745–748.

[17] R.H. Perry, D.W. Green, Perry's Chemical Engineers Handbook, vol. 2, Sci. Press, Beijing, 2001.

[18] J. Sun, M.L. Pantoya, S.L. Simon, Thermochim. Acta 444 (2006) 117–127.

[19] M.L. Pantoya, J.J. Granier, J. Therm. Anal. Calorim. 1 (2006) 1–7.